Performance improvement by advanced high field side pellet refueling in ASDEX Upgrade

P. T. Lang*, A. Lorenz, M. Reich†, R. Dux, J. Gafert, V. Mertens,
H.W. Müller, J. Neuhauser, K.F.Renk†, ASDEX Upgrade Team

Max-Planck-Institut für Plasmaphysik, EURATOM Association,
Boltzmannstr. 2, 85748 Garching, Germany
† *Institut für Experimentelle und Angewandte Physik,*
NWF II, Universität, 93040 Regensburg, Germany
* *Corresponding author; e-mail: ptl@ipp.mpg.de*

1. Introduction

A tokamak's operational area accessible by gas puff refueling can be enhanced by injection of cryogenic hydrogen isotope pellets. When pellet particles are deposited sufficiently deep inside the plasma core, less confinement degradation takes place with increasing density, allowing e.g. sustainment of the H-mode even beyond the Greenwald density $\bar{n}_e^{Gw}$ [1]. In hot plasmas, the pellet ablation cloud becomes subject to a strong curvature drift towards the magnetic low field side. This drift influences the pellet penetration and the particle deposition profile, causing strong improvement in penetration and deposition when launching the pellet from the magnetic high field side (HFS) instead of the low field side (LFS). Plasma refueling experiments applying HFS pellet launch indeed showed favourable performance with respect to density and energy [2]. However, with currently available launch scenarios in large tokamaks, the resulting deposition profiles are still significantly off-axis. Therefore, the adiabatic pellet induced density jump in the plasma is followed by a phase of strong particle and energy losses, causing some plasma energy reduction during density ramp up. Increasing the particle deposition depth d_p is expected to yield reduction of the post-pellet energy and particle losses by raising the decay time τ^* of the pellet induced density surplus. For a given constant diffusion coefficient the residence time of pellet deposited particles scales as ${d_P}^2$. In H-mode discharges discontinuous transport modifications by ELMs change this relation, making deeper deposition even more favourable. For further improvement by deeper particle deposition, two options are currently under development: (i) using a higher pellet launch speed, (ii) reducing the local pellet ablation rate. Applying option (i) by operating an improved pellet guiding system capable of realizing enhanced launch speed for HFS injection [3] are reported here.

2. Experimental setup

The pellet injection scheme used in the present study employs a looping geometry, as displayed in figure 1. This looping consists of three elliptic parts: a) a funnel to collect the scattered pellets from the centrifuge, b) a guiding tube element including a diagnostic section and c) a guiding track segment in the torus port to link up with the plasma. With this setup in a preliminary sprint version pellets at v = 240 and 560 m/s became available for plasma injection, the poloidal injection angle set to about 72^o with respect to the horizontal midplane.

In the experiments target plasmas with $I_P = 1MA$, $B_t = 2.7T$, $q_{95} = 3.8$ were run in the lower single null divertor configuration with elongation $\kappa = 1.6$ and with low triangularity (averaged $\delta < 0.2$). The cryopump with $100m^3/s$ pumping speed was applied together with the turbomolecular pumps ($14m^3/s$) for efficient particle exhaust. Discharges prefilled with hydrogen gas were driven by approx. $6MW H_0$ NB injection into a stationary ELMy H-mode phase, the base density before (and after) the pellet sequence was adjusted

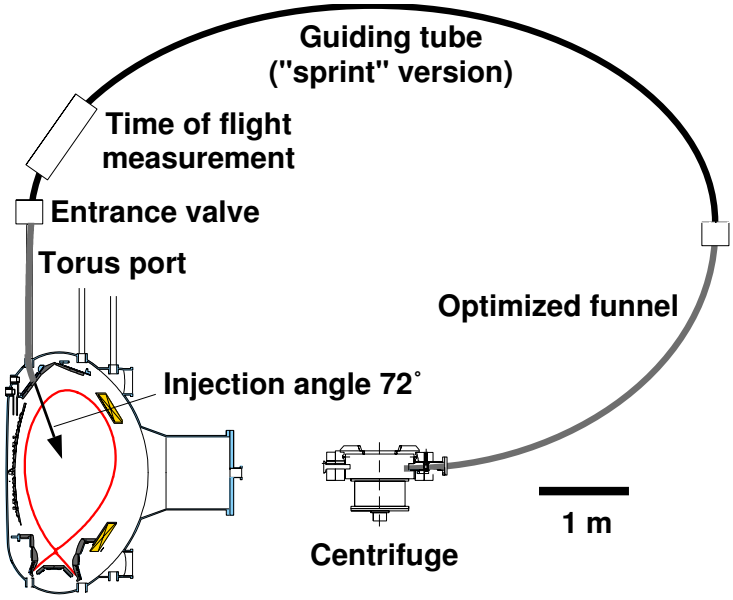

Figure 1: *Schematic view of the preliminary pellet injection system at ASDEX Upgrade for high speed launch from the torus inside. Pellets leaving the centrifuge are first collimated in the funnel section and then guided through the looping guiding tubes into the plasma vessel. Pellets leave the guiding tube at an angle tilted by 72° to the horizontal plane, aiming at the plasma centre for a standard plasma configuration.*

to approx. $3.5 \times 10^{19} m^{-3}$ by hydrogen gas puffing. Pre-programmed sequences of cubic $(2mm)^3$ deuterium pellets were injected at moderate repetition rates into steady state phases of the discharges. A full set of diagnostics was in operation, some run in an adapted setting to record density and temperature profiles at high temporal resolution. This way, pellet deposition profiles were obtained from density profiles measured before and almost immediately after pellet injection.

3. Results

First, the impact of the increased pellet velocity on penetration was investigated. From the total D_α radiation emitted during the ablation process an estimate of the penetration depth λ_{pen} was performed by assuming constant pellet velocity and penetration along the ideal injection path. A statistical analysis yielded an averaged penetration depth of λ_{pen} of $18.2 \pm 1.7cm$ for 240 m/s pellet velocity and 24.0 ± 1.1 for the 560 m/s pellets. The result was confirmed by the soft X-ray time traces displaying distinguished emission pulses in respective penetration zones and by video observation of the injection path.
For the relative improvement of λ_{pen} with pellet velocity, very good accordance of the data with the empirical multi machine IPADBASE [4] scaling derived for LFS pellets is found when taking into account the slightly different masses. As all other important plasma parameters were virtually unchanged in the experiment, this scaling yielding $\lambda_{pen} \sim m_P^{5/27} \times v_P^{1/3}$ predicts a ratio of $\frac{\lambda_{pen/560}}{\lambda_{pen/240}} = 1.27$, rather close to the experimental value of 1.32. For a comparison of absolute penetration depths, the different injection geometry has to be taken into account, as the IPADBASE scaling was derived using data for horizontal LFS injection towards the plasma center. Comparing penetration with respect to the magnetic configuration this way turned out to agree well with the scaling. Deeper penetration at higher pellet velocity was found to be correlated to the pellet induced particle deposition profiles. This is shown in figure 2, where particle deposition

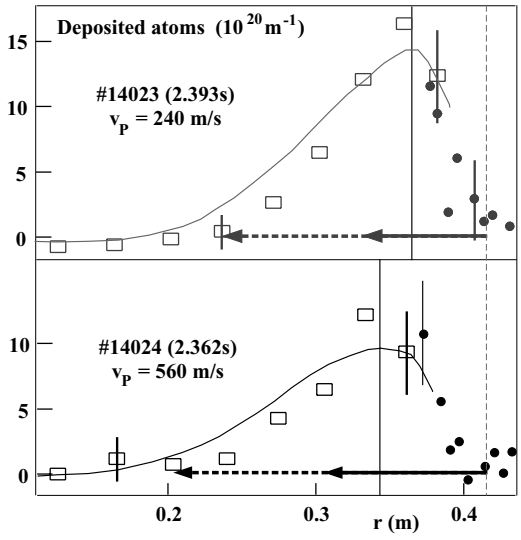

Figure 2: *Particle deposition profiles for v_p = 240 m/s and 560 m/s: DCN laser interferometer deconvolution including Li beam data (solid lines), Thomson scattering (squares) and LFS reflectometry (circles). Pellet penetration mapped onto the outer horizontal midplane (solid arrow), maximum possible pellet particle deposition depth due to curvature drift (dashed arrow).*

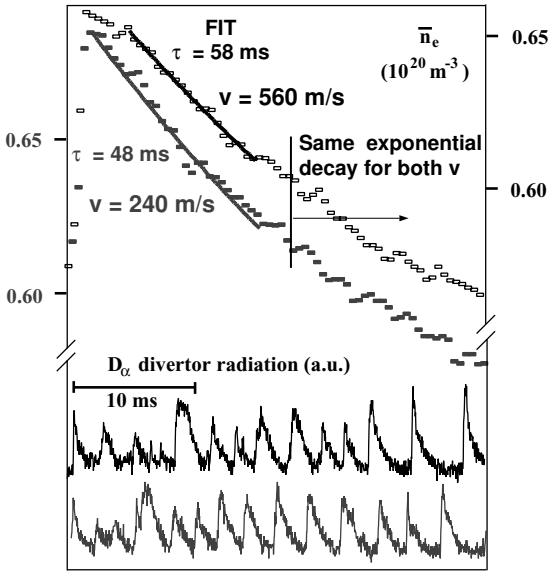

Figure 3: *Evolution of line averaged density (top) and D_α radiation from the outer divertor strike point area (bottom) during injection of single pellets comparing v_p = 240 m/s with 560 m/s. Both pellets having similar size meet almost identical target plasma conditions.*

profiles deconvoluted from DCN and Li (solid line) before and within 2 ms after the pellet ablation are plotted for both pellet velocities. Also, the deposition profile determined from Thomson data (squares) and reflectometry measurements at the plasma high field side (dots) are given, confirming the profile evolution. Solid arrows indicate the averaged pellet penetration, mapped onto the horizontal outboard axis as mentioned before. For both velocities a clear shift of particle deposition to the centre is visible with respect to the ablation region. Particle displacement beyond the region of direct ablation can be attributed to the plasmoid curvature drift, already observed previously [2,5,6]. Dashed arrows visualize the maximum deposition depth pellet particles can achieve by the drift, agreeing well with the end of the deposition profile. Therefore, higher pellet velocity not only causes deeper pellet penetration but also particle deposition deeper inside the plasma column. This shows that higher pellet injection speeds have the potential for deeper HFS particle fueling.

Having proven that higher HFS launch speed can create more favourable particle deposition profiles, a closer look was taken on the pellet fuelling behaviour with respect to global plasma parameters. In particular, the prompt particle and energy loss during the first phase after pellet injection characterized by ELM bursts and a fast density decay was analyzed. As aimed for, the ELM induced losses were mitigated at the higher pellet velocity. Figure 3 shows the temporal evolution of line averaged density $\bar{n}_e$ and the D_α radiation from the outer divertor area following pellet launch at the two velocities for otherwise virtually identical conditions. In the case of the higher pellet velocity, the onset of strong pellet induced ELMs shows a remarkable delay compared to the slower pellet. Pellet induced ELMs are generally longer and stronger than "background" ELMs, corre-

lated to a significant plasma particle inventory reduction after heavy particle losses from the edge region. Delayed onset of strong particle losses from the edge at higher pellet velocities is confirmed by reflectometry measurements performed at the plasma high field side. Sustainment of the pellet enhanced density and corresponding modifications of the local density gradients near the plasma edge was found to last 8 to 12 ms for $v_P = 560$ m/s and approx. 6 ms for $v_P = 240$ m/s [7]. Correlated to the strong particle losses during the pellet induced ELMs, a significant reduction of the plasma energy was observed. This behaviour has already been documented at ASDEX Upgrade and JET and can be correlated to the boundaries of the accessible operational area [1]. The delayed onset of enhanced ELM activity upon injection of the faster pellets results also in a reduced magnitude of W_{MHD} losses. A statistical analysis yielded an averaged $\bar{n}_e$ decay time for the ELM burst phase of $49.0 \pm 2.2ms$ for the slow and $58.2 \pm 1.3ms$ for the fast pellets. After this first fast density decay phase, slow density reduction towards the background plasma density with a time constant of about $85ms$ was found in both cases. The additional power loss caused by the pellet induced ELMs during this first phase was determined as $1.05 \pm 0.18MW$ for the slow and $0.84 \pm 0.14MW$ for the fast pellets. After termination of the pellet induced ELMs, W_{MHD} starts to recover to its initial unperturbed value. It should be noted that in this analysis a few pellets showing strong MHD activity in the post-pellet phase were excluded. It seems, the faster pellets showed a somewhat higher probability of triggering sawteeth. The occurrence of a sawtooth in the post-pellet phase causes somewhat increased particle and energy losses. This behaviour is attributed to the deeper penetration and particle deposition of the faster pellets. Reasonable q-profiles as required for example in advanced scenarios should aid to avoid this problem.

4. Outlook

The pellet system at ASDEX Upgrade is currently set up in its final scheme, aiming at still higher pellet speeds and better fuelling performance. The highest available velocity should yield the least convective loss power and realise the best operational boundaries for steady state pellet injection. Further improvement by reducing the ELM related losses seems feasible by pellet sequencing; short high repetitive pellet phases interrupted by recovery phases where the initial plasma energy can be regained with still pellet induced density enhancement. This approach, relying on the ratio particle/energy confinement time > 1 has been shown to allow dynamic operation even beyond steady state operation [1]. A combination of a density ramp up phase using the best achievable steady state performance followed by a phase applying pellet sequencing for density controlling should then form the most advanced pellet refuelling scenario. Refuelling investigations towards this goal are envisaged now with the pellet injection system in the final fully optimised setup at ASDEX Upgrade with the modified divertor IIb.

References

[1] P.T. Lang et al., in Controlled Fusion and Plasma Physics (Proc. 27th Eur. Conf. Budapest, 2000), P3.045

[2] P.T. Lang et al., Phys. Rev. Lett. **79** (1997) 1487.

[3] P.T. Lang et al., Nucl. Fusion, *in press.*

[4] L.R. Baylor et al., Nucl. Fusion **37** (1997) 445.

[5] L.R. Baylor et al., in Controlled Fusion and Plasma Physics (Proc. 26th Eur. Conf. Maastricht, 1999), P1.048

[6] T.T.C. Jones et al., in Controlled Fusion and Plasma Physics (Proc. 27th Eur. Conf. Budapest, 2000), OR04

[7] S. Vergamota et al., APS Conference, Quebec (2000)